



UNIVERSITY OF SEVILLE

Master Thesis

*Evaluating the modulation of the intracellular
production of H₂S in the functionality and metabolic activity of primary
cultures of pancreatic islets*

Master in Biomedical Research

Andalusian Center of Molecular Biology and Regenerative Medicine



21 February 2022 – 5 September 2022

Inmaculada Pino Pérez

In Seville, 5 of September of 2022

Tutor: Alejandro Martín-Montalvo Sánchez

Co-tutor: Iván Valle Rosado

Date of the defense: 22 of September of 2022

PINO PEREZ
INMACULA
DA -
30266695Y
Firmado digitalmente por
PINO PEREZ
INMACULADA -
30266695Y
Fecha: 2022.09.04
14:02:12 +02'00'

MARTIN-
MONTALVO
SANCHEZ
ALEJANDRO -
28806216G
Firmado digitalmente
por MARTIN-
MONTALVO SANCHEZ
ALEJANDRO -
28806216G
Fecha: 2022.09.05
09:49:09 +02'00'

VALLE
ROSADO
IVAN -
28767361L
Firmado digitalmente por
VALLE ROSADO
IVAN - 28767361L
Fecha: 2022.09.04
19:54:15 +02'00'

Abstract

Diabetes Mellitus is a metabolic disease characterized by hyperglycaemia that currently affects one in ten people worldwide. Uncontrolled Diabetes is associated with long-term damage and dysfunction and failure of different organs. Although there are therapies for the treatment of diabetes, they are not strongly effective. In order to develop an appropriate therapy for diabetes, we are studying the modulation of the intracellular production of the gasotransmitter hydrogen sulfide (H₂S) in pancreatic islets using a H₂S donor (compound α). Mice treated with two doses (5 and 10 μ M) of compound α showed increased metabolic activity and oxygen consumption rate in islets exposed to high concentrations of glucose (22 mM) when compared with the untreated control, suggesting that mitochondria are one of the main targets of H₂S effects. Importantly, compound α showed increased insulin secretion under high glucose (22 mM) conditions. Lentiviral-mediated overexpression of Cystathionine-beta-synthase and Cystathionine-gamma-lyase, main enzymes that synthesise endogenous H₂S, in primary pancreatic islets also showed increased metabolic activity. Taken together, these data indicate that compound α , a H₂S generator, increases metabolic activity and produces greater insulin secretion in murine primary pancreatic islets.

INDEX

I.	Antecedents	1
II.	Objectives.....	7
III.	Material and Methods.....	8
IV.	Results and Discussion.....	14
V.	Conclusions	24
VI.	Bibliography.....	25

I. Antecedents

The incidence of Diabetes Mellitus (DM) is fast increasing worldwide¹. This endocrine and metabolic disease is defined by the American diabetes Association as a group of metabolic diseases characterised by hyperglycaemia resulting from insulin secretion deficiency or by its compromised biological function^{2,3}. Over the last few years, the number of people with this multifactorial disease has increased rapidly. According to the International Diabetes Federation (IDF), in 2021 approximately 537 million adults (20-79 years) were living with DM and the total number of people living with diabetes is projected to rise to 643 million by 2030 and 783 million by 2045. DM is traditionally divided into type 1 diabetes (T1D) and type 2 diabetes (T2D), although other types of DM also exist (American diabetes association, 2021). In most cases, type 1 diabetic patients have a complete lack of insulin due to a failure of β -cell-specific self-tolerance by T-lymphocytes. The lack of self-tolerance sets in motion an autoimmune attack and the elimination of insulin-producing cells in the endocrine pancreas⁴. This type of DM commonly manifests during childhood⁵. On the other hand, T2D is a non-insulin-dependent DM^{6,7}.

Insulin-producing cells (β -cell) are one of the main types of endocrine cells of the endocrine pancreas⁸. The pancreatic endocrine cells are settled into clusters, called islets of Langerhans and there are five principal types: the β cells (insulin-producing cells), the α cells (glucagon-producing cells), the δ cells (somatostatin-producing cells), the ϵ cells (ghrelin-producing cells) and PP cells (pancreatic polypeptide-producing cells)⁹. These pancreatic cells clusters are highly vascularized, and this allows that the insulin is secreted into the circulation to target the insulin-sensitive organs, such as the liver or the skeletal muscle¹⁰. β and α cells play an important role in glucose sensing and the maintenance of glucose homeostasis. Specifically, pancreatic β -cells sense changes in plasma glucose levels and are responsible for the synthesis and secretion of insulin¹¹.

In type 2 diabetics, insulin-producing cells do not fabricate enough insulin, or they cannot secrete it effectively. These effects result in high blood glucose levels and can be due to influencing factors such as heritable genetic correlation (40% of first-degree relatives of patients with T2D develop DM) or environmental factors (sedentary lifestyles, unhealthy diet, obesity or ageing)¹². Nowadays, this complex disease is diagnosed by measuring glucose in blood under fasting conditions or after challenging the body with a glucose load (glucose tolerance tests)¹³. Moreover, in the diagnosis of DM a determination of glycated haemoglobin

is normally used, which allows a determination of long-term hyperglycaemia. Nevertheless, despite being relatively easily diagnosed, in Europe over 1 in 3 adults (36%) living with DM are undiagnosed (IDF, 2021). DM that is not well controlled can have an important impact on mortality and morbidity, including being a health risk for obesity, stroke, renal dysfunction, heart and vascular diseases, blindness, and neuropathy^{14,15}. In fact, DM was responsible for 6,7 million deaths in 2021 (IDF, 2021). Current therapies for the different types of DM are not, in general, highly effective. Therefore, it is necessary to develop novel strategies for managing DM. The lifestyle strategies frequently include ordinary physical activity, avoid smoking, avoid obesity and the use of healthy diet with low glycaemic index and high fibre content¹⁴. Symptoms of DM can be treated by pharmacological therapy with exogenous insulin and other molecules as glucagon-like peptide-1 (GLP-1) receptor agonists, sodium-glucose cotransporter-2 (SGLT2) inhibitors, thiazolidinediones and sulfonylurea derivatives, but these therapies are, in the majority of the cases, not very successful¹⁶. For this reason, it is necessary to bet on new strategies for this complex disease. On this point, there is evidence that hydrogen sulfide (H₂S) is produced endogenously in different organs by enzymatic and non-enzymatic production. The non-enzymatic production of H₂S is responsible for approximately 10-50% of total H₂S production. The enzymatic production of H₂S is organ-specific. H₂S endogenous production plays a regulatory role in physiological processes, such as adipogenesis and adipose tissue metabolism which are promoted by endogenous H₂S¹⁷. Previous reports indicate that H₂S could be endogenously produced in islet β -cells, liver and adipose tissue, suggesting that this molecule could play a significant role in the survival or functionality of metabolic tissues. Furthermore, it has been found that H₂S might be involved in the regulation of insulin sensitivity and insulin secretion. In addition, further research has indicated that H₂S levels are decreased in diabetic subjects when compared with healthy individuals, suggesting a link between H₂S and diabetogenesis¹⁸.

In mammal tissues, enzymatic production occurs primarily through the actions of four enzymes¹⁹: Cystathionine-beta-synthase (CBS), Cystathionine-gamma-lyase (CSE or CTH), 3-mercaptopyruvate sulfurtransferase (3-MST) and cysteine aminotransferase (CAT)²⁰ (Figure 1). CBS and CTH catalyse the production from L-cysteine and/or homocysteine, while 3-MST can catalyse 3-mercaptopyruvate to produce H₂S¹⁹.

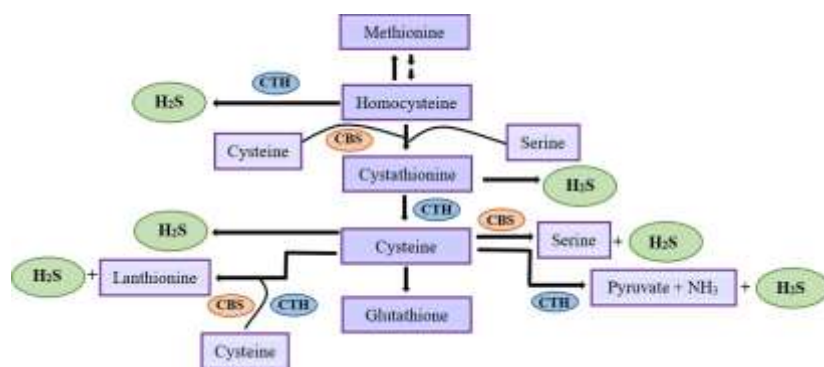


Figure 1. H₂S generation via enzymatic pathway.

Modified from Zhu et al., 2020²⁰.

The distribution of these enzymes is tissue specific¹⁸. CTH has its main role in the production of H₂S in the peripheral system (pancreas, liver, adipose tissue, cardiovascular system, and respiratory system), whereas CBS is abundantly expressed in the central nervous system²¹. Furthermore, in pancreatic β -cells it has been discovered a generation of H₂S through CBS (exocrine and endocrine pancreatic cells) and/or CTH (exocrine pancreatic cells)¹⁸. 3-MST has an important role in the production of H₂S in those tissues with high cysteine concentration, such as the kidney, but its principal expression is in the gastrointestinal tract²².

In addition to the enzymatic production, H₂S is produced via a non-enzymatic endogenous generation that is less well understood. In this H₂S production, the reducing power (NADPH) that is generated by different metabolic pathways, including glycolysis or phosphogluconate, is used to reduce oxidized glutathione (GSSG) to glutathione (GSH) which allows the generation of H₂S by the reduction of polysulfides (Figure 2)²³.

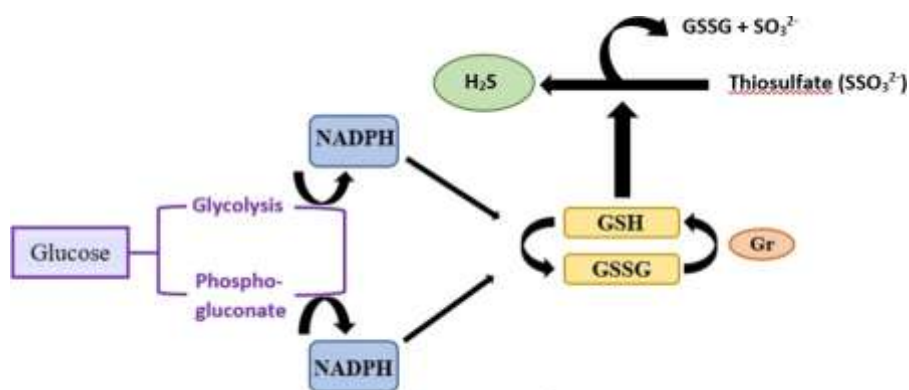


Figure 2. H₂S generation via non-enzymatic pathway.

Modified from Kolluru et al., 2013²³.

Despite of been known for its toxicity over the years, H₂S, a “toxic gas with strong odor of rotten eggs” has gone from a toxic gas to a signalling molecule²⁴, which was first described as an endogenous neuromodulator by Abe and Kimura in 1996²⁵. H₂S is a gasotransmitter that has the ability to diffuse freely through cells membranes²⁶ and in physiological concentrations this molecule mediated important biological actions as vasorelaxation, changes in brain neurotransmission and the effect on K⁺ATP channel²⁷.

Evidence suggests that physiological effects of H₂S are linked to the post-translational modification S-Sulfhydration of target proteins in cysteines (persulfidation). In this reaction, H₂S transfer a sulfhydryl group (-SH) to a cysteine residue of a protein and this contribute to the modification of functions, stability, and localization of cells²⁸. This post-translational modification favoured by H₂S could be an important signalling mechanism of metabolism.

Alternatively, H₂S effects might originate from the action of Sulfide Quinone Oxidoreductase (SQOR). SQOR is a mitochondrial inner membrane-anchored flavoenzyme which catalyses the first step in the mitochondrial H₂S oxidation pathway²⁹. This oxidation by SQOR is coupled to the reduction of the coenzyme Q³⁰. In low concentrations (<20 μM) H₂S stimulates mitochondrial respiration donating an electron to the electron transport chain (ETC) resulting from its oxidation by SQOR. Specifically, the electrons are captured by ubiquinone and are incorporated into the ETC at the level of Cytochrome C reductase (Complex III)³¹. This activity can stimulate oxidative phosphorylation and ATP production in the cell²².

In the field of DM, different implications of H₂S have been discovered. Several studies have demonstrated that DM is associated with lower circulating concentrations of H₂S^{32,33}. Several reports have showed in patients and experimental animals (rats and mice) that diabetic individuals have lower circulating H₂S concentrations than age-matched non-diabetic individuals³⁴.

Focusing on pancreatic β-cells, Zhang et al., 2014, have found that the effect of increased H₂S production could limit insulin secretion in Zucker diabetic fatty rats. The increase in H₂S production is due to the enzymatic action of CTH (main producer of H₂S in the peripheric system, which includes the endocrine pancreas) because the addition of an enzymatic inhibitor of CTH recovers the normal insulin secretion¹⁸.

Pancreatic β-cells work as sensors of glucose circulation levels. When circulating glucose concentrations are high, β-cells secrete insulin, and this mechanism is mediated by the ATP-dependent inhibition of K^{ATP} channels (Figure 3). In β-cells glucose enters via GLUT2

transporter. Within the cells, glucose enters glycolysis, an ATP-producing pathway. Moreover, the last metabolite of glycolysis, pyruvate, can enter into the mitochondria to be catabolized to CO₂ with the subsequent generation of reduction power. This reduction power is used to feed the mitochondrial ETC, ultimately producing the generation of ATP in the mitochondrial Complex V. As a result of glycolytic and mitochondrial ATP generation the intracellular ATP/ADP ratio increases³⁵. ATP induces K^{ATP} channel inhibition, β-cell depolarization, and voltage-dependent calcium channel opening. All this process leads to the release of insulin-containing vesicles³⁶. Insulin secretion would be stimulated by H₂S through depolarization of mitochondrial membrane potential (MPP) and causing an increase in Ca²⁺ release from mitochondria. This increased Ca²⁺ ultimately leads to an increase in insulin secretion³⁷.

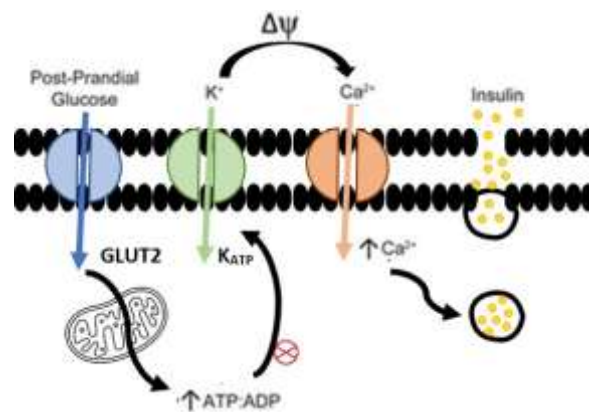


Figure 3. Insulin secretion process in pancreatic beta cells.

Modified from Szeto et al., 2018³⁶.

On the other hand, H₂S might be also implicated in diabetogenic processes by altering the insulin secretion mechanism. H₂S endogenously produced, by opening the K^{ATP} channel of vascular smooth muscle cells, produces vasorelaxation³⁸. Due to the importance of β-cell K^{ATP} channels in regulating insulin secretion and considering these effects on vascular smooth K^{ATP} channels, this process could be the responsible of its function as an endogenous modulator of insulin secretion. This process might constitute an important mechanism for the fine control of insulin secretion³⁴. Interestingly, Bełtowski et al., 2018 demonstrated that some H₂S donors such as NaHS reduced insulin secretion stimulated by glucose⁴⁰. Supporting this, recent results from Dr. Alejandro Martín Montalvo's research group, have shown that mice fed during 4 months with the H₂S donor compound α , show decreased insulin in circulation during an Oral Glucose Tolerance Test (OGTT). Moreover, results in Insulin Tolerance Test (ITT) indicate low glucose levels in mice treated with compound α . The effects on insulin levels on circulation promoted by compound α could be interpreted as an adaptation to the high sensitivity to insulin

produced by H₂S in insulin target tissues such as liver, white adipose tissue or skeletal muscle. Considering these results, it is tempting to speculate that long term treatments with H₂S generators would modify glucose-promoted insulin secretion in pancreatic beta cells and increase the sensitivity to insulin in target tissues, avoiding hypoglycaemic episodes³⁹. To achieve these beneficial effects, H₂S donors may be attractive options for the treatment of DM. In this project, we set out to investigate the potential of the modulation of H₂S production in the functionality of the endocrine pancreas. We modulated the intracellular H₂S production using an H₂S donor, named compound α , as well as modulating the expression of the main H₂S-producing enzymes in primary culture of murine pancreatic islets.

II. Objectives

The main objective of this Master thesis is to explore and evaluate the effectiveness of an innovative strategy for the potential development of a new therapy for the treatment of DM. More specifically, we aim to determine the effects of the increase in the intracellular production of H₂S, using an H₂S donor (compound α) in mitochondrial function and insulin secretion in primary cultures of the pancreatic islets.

III. Material and Methods

Animals

4-8-week-old male mice (C57/BL6J) were used to perform this research. Mice experimentations were approved by the CABIMER Animal Committee and performed in accordance with the Spanish law on animal use RD 118/2021.

Reagents and drugs

Product	Vendor	Catalog Number
Collagenase from Clostridium histolyticum	Sigma-Aldrich	C9263-1G
Islets isolation solution	Handmade (NaCl 115mM, KCl 5mM, NaHCO ₃ 10 mM, MgCl ₂ 1,1 mM, NaH ₂ PO ₄ 1,2 mM, HEPES 25mM, CaCl ₂ 2,56mM, 90mg/2 mice of Glucose and 0,5-1gr/2 mice of Bovine Serum Albumin V (BSA)) supplemented with 0,008gr/mice of collagenase from Clostridium histolyticum. pH 7,4)	
HEPES	Sigma-Aldrich	H4034
DMSO	Sigma-Aldrich	D2650
BSA	VWR	P6154
Glutamine	Sigma-Aldrich	G7513
Sodium pyruvate	Gibco	11369-039
β-mercaptoethanol	Gibco	31350-010
PBS	Sigma-Aldrich	D8537
Penicilin/Streptomycin	Gibco	15140122
RPMI 1640	Sigma-Aldrich	R0883
Fetal bovine serum (FBS)	Sigma-Aldrich	F7524
Seahorse XF Calibration Buffer	Agilent Technologies	100840-000
XF DMEM assay medium	Agilent Technologies	103575-100
MA Media	Handmade (XF DMEM assay media was supplement with 3 mM glucose and 1 % FBS)	
Oligomycin	Merk Millipore	495455
FCCP	Sigma-Aldrich	C2920
Rotenone	Santa Cruz Biotechnology	SC-203242
Antimycin A	Sigma-Aldrich	A8674
Glucose	VWR	24379-363

Thiazolyl blue tetrazolium bromide, 98%	Alfa Aesar	L11939
MTT solubilization solution	Handmade (SDS 10% + HCL 0,01M)	
Krebs-Ringer Bicarbonate HEPES buffer (KRBH-BSA)	Handmade (140 mM NaCl, 3.6 mM KCl, 0.5 mM NaH ₂ PO ₄ , 0.5 mM MgSO ₄ , 1.5 mM CaCl ₂ , 2 mM NaHCO ₃ , 10 mM HEPES, 0.1% BSA. pH 7,4)	
Trypsin- EDTA 10X	Gibco	15400054
Hank's Balanced salt solution	Sigma-Aldrich	H9394
Dulbecco's Modified Eagle Medium D5796 (DMEM D5796)	Sigma-Aldrich	D5796
CTH Lentiviral Vector (Human)	Applied Biological Materials (abm)	170620610395
CBS Lentiviral Vector (Human)	Applied Biological Materials (abm)	151190610395
pMD2.G Plasmid	Addgene	12259
psPAX2 Plasmid	Addgene	12260
RPMI 1640 Complete Media	Handmade (RPMI 1640 media supplemented with 10% FBS, Pen-strep, 2 mM glutamine, 1 mM sodium pyruvate, 50 μM β-mercaptoethanol and 10 mM HEPES)	
RPMI 1640 Media	Sigma-Aldrich	R0883
Ultra Sensitive Mouse Insulin ELISA Kit	Crystal Chem	90080
Qiagen RNeasy Micro kit	Quiagen	74004
iScript cDNA Synthesis Kit	BIO-RAD	1708891
RT-PCR SYBR Green Kit	BIO-RAD	1725124
0,5X Trypsin-Ethylenediaminetetraacetic acid	Handmade (aliquots of 0,5% Trypsin-EDTA 10X (5000 mg/l; 9,6mM EDTA) are in Hanks Balanced Salt Solution 1X to obtain a final concentration of 0,5X Trypsin-EDTA (250mg/l; 0,48mM EDTA)	

Primer	Vendor	Sequence (Fw)	Sequence (Rw)
RPS29	Biomol	5'-GGA GTC ACC CAC GGA AGT T-3'	5'-CAT GTT CAG CCC GTA TTT GC-3'

GLUT2	Biomol	5'-TTG ACT GGA GCC CTC TTG ATG-3'	5'-CAC TTC GTC CAG CAA TGA TGA-3'
INS1	Biomol	5'-CCT GTT GGT 5' GCA CTT CCT AC-3'	5'-TGC AGT AGT TCT CCA GCT GC-3'
INS2	Biomol	5'-GCA GCA CCT TTG TGG TTC CC-3'	5'-TGC AGT AGT TCT CCA GCT GG-3'
GCK	Biomol	5'-CTT CAC CTT CTC CTT CCC TG-3'	5'-ATC TCA AAG TCC CCT CTC CT-3'
CBS (for Mice CBS overexpression)	Biomol	5'-AGA GAC AAC TGG AGA AGG GC- 3'	5'-CGT ATG CGG TCC TTC ACA C-3'
CBS Lentivirus (for Human CBS overexpression)	Biomol	5'-CTT CCC GGT GCT GTG GTA-3'	5'-CAT GCT CTC GCT CCT GCT-3'
CTH (for Mice CTH overexpression)	Biomol	5'-TTG GAT CGA AAC ACC CAC AAA-3'	5'-AGC CGA CTA TTG AGG TCA TCA-3'
CTH Lentivirus (for Human CTH overexpression)	Biomol	5'-TGT GGA TGA GAG GGC AGC-3'	5'-ATG GGC CTG GTG TCT GTT-3'
SQOR	Biomol	5'-TGG GGA CCT TCA GGA TCT AA-3'	5'-GGA CTG GAG ACA ACA GTG ACC-3'
GFP	Biomol	5'-GTT GCT GCG GAT GAT CTT GT-3'	5'-AAC ACC CGC ATC GAG AAG TA-3'

Pancreatic islets procurement and culture

Mice were sacrificed by cervical dislocation and pancreatic islets were isolated by intraductal collagenase perfusion as previously described⁴⁰. In brief, islets were perfused with islets isolation solution (NaCl 115mM, KCl 5mM, NaHCO₃ 10 mM, MgCl₂ 1,1 mM, NaH₂PO₄ 1,2 mM, HEPES 25mM, CaCl₂ 2,56mM, 90mg/2 mice of Glucose and 0,5-1gr/2 mice of Bovine Serum Albumin V (BSA)) supplemented with 0,008gr/mice collagenase from *Clostridium histolyticum* (Sigma).

Before culture islets were washed with Phosphate Buffered Saline (PBS) containing 100U/ml penicillin and 100 µg/ml streptomycin (Pen-strep) to minimize post-isolation contaminations. Afterwards, isolated islets were cultured overnight in RPMI 1640 media supplemented with

10% FBS, Pen-strep, 2 mM glutamine, 1 mM sodium pyruvate, 50 μ M β -mercaptoethanol and 10 mM HEPES (RPMI complete media).

The following day, healthy islets were separated and treated with three different conditions: DMSO 0,1% as a control, compound α 5 μ M and compound α 10 μ M (in DMSO).

Oxygen consumption rate and extracellular acidification of the media

Mitochondrial function was assessed in islets using an Agilent Seahorse XF24 according to the instructions of the manufacturer (Agilent Technologies). XF DMEM assay media was supplemented with 3 mM glucose and 1 % FBS (MA Media) to run the whole islets and the Seahorse XF Sensor Cartridge was hydrated with Seahorse XF Calibration Buffer at 37 °C overnight.

The day of the assay, 30 islets per well were placed in Agilent Seahorse XF24 Islet Capture Microplates along with 500 μ L of MA Media. Islets were captured with a capture screen in each well. Then, the oxygen consumption rate (OCR) and the extracellular acidification rate (ECAR) were measured. OCR and ECAR were determined in basal conditions and through consecutive injections of glucose (20 mM), oligomycin (5 μ M), carbonyl cyanide 4-(trifluoromethoxy) phenylhydrazone (FCCP; 1 μ M) and rotenone (5 μ M) with antimycin A (5 μ M). The durations of the injections were basal conditions 3 cycles (1 cycle: mix, wait and measure), glucose 5 cycles, oligomycin 5 cycles, FCCP 5 cycles and rotenone with antimycin A 7 cycles.

Thiazolyl blue tetrazolium bromide (MTT) assay

The islets cell metabolic activity was determined using the Cell Proliferation kit according to the recommendations of the manufacturer (Roche, Spain). Firstly, 30 islets/well of each condition were cultured into a 24-well plate. MTT assay reagent (60 μ L thiazolyl blue tetrazolium bromide) was added to the medium, and incubated at 37 °C, 5% CO₂ for 2 hours before adding 600 μ L MTT solubilization solution. The next day, the Optical density was determined at 575 nm with a reference wavelength of 690 nm using a Varioskan Flash spectrophotometer (Thermo Scientific, Spain).

Insulin Secretion

Groups of 10 islets of each condition (DMSO 0,1%, Compound α 5 μ M and Compound α 10 μ M) were washed in Krebs-Ringer Bicarbonate HEPES buffer (KRBH-BSA) (140 mM NaCl, 3.6 mM KCl, 0.5 mM NaH₂ PO₄, 0.5 mM MgSO₄, 1.5 mM CaCl₂, 2 mM NaHCO₃, 10

mM HEPES, 0.1% BSA) and incubated for 1 h at 37°C in KRBH-BSA solution containing 3mM glucose (KRBH-BSA-Glucose) and supplemented with their treatment condition. Then, ten size-matched islets per condition were incubated for 30 min at 37°C with either 3 mmol/l glucose (low glucose), 22 mmol/l glucose (high glucose) or 20 mmol/l KCl. Secreted and total insulin were quantified using an Ultra Sensitive Mouse Insulin ELISA Kit according to the manufacturer's instructions (Crystal Chem).

RNA Extraction and RT-PCR

Quiagen RNeasy Micro kits were used for the extraction of total RNA from the pancreatic islets according to the instructions of the manufacturer (Quiagen). After extraction, the quantification of the RNA was done using a DS-11 Spectrophotometer/ Fluorometer (DeNovix). To perform the real-time PCR, single-stranded cDNA was synthesized with the iScript cDNA Synthesis Kit according to the instructions of the manufacturer (BIO-RAD). The gene-specific primers (RPS29, GLUT2, INS1, INS2, GLUCOKINASE, CBS, CTH, SQOR, GFP) were obtained from Biomol and the RT-PCR was performed on a QuantStudio 7 Pro using the RT-PCR SYBR Green Kit according to the instructions of the manufacturer (BIO-RAD). Expression levels of the housekeeping RSP29 gene were used for normalization.

Lentivirus Amplification and Purification

Lentivirus production was done using 5×10^6 Hek293T cells that were seed in a 100mm petri dish for virus package for 24 hours. The following day, cells were transfected with 3 plasmids: 1) 2,5 µg of interest plasmid (CBS, CTH, CONTROL), 2) 1 µg of envelope plasmid (pMD2.G), 3) 1,5 µg of capsid plasmid (psPAX2). The transfection was performed following the protocol of LipoD293. LipoD293 is diluted with Dulbecco's Modified Eagle Medium D5796 (DMEM D5796) supplemented with FBS 10%, Pen/Strep 1X y Glutamine 10% and allows transfection by making pores in cells. After transfection, for 72 hours lentivirus were harvested and then purified using a 0,45 µm Whatman Puradisc filter and concentrated by ultracentrifugation in a Optima XPN-100 Ultracentrifuge (Beckman Coulter, United States) at 22000 rpm for 2 hours at 4°C. Virus particles were resuspended in DMEM D5796, distributed in aliquots according to the conditions and stored at -80°C. Hek293T cells were transduced with the viral particles obtained and the viral titer was estimated by flow cytometry analysis (FAC-SCalibur, BD Biosciences, Spain). This analysis allows to determine the Plaque Forming Units/mL (PFU/mL) based on GFP (Green Fluorescent Protein) emission.

Islets Infection

After isolation by collagenase digestion, islets were picked and cultured in a petri dish with RPMI 1640 for 3 hours at 37°C. After the incubation, islets were separated in the same number in three 15mL falcon tube, for separate each lentivirus condition: lentivirus control, lentivirus CBS and lentivirus CTH. Subsequently islets were incubated in 0,5X Trypsin-Ethylenediaminetetraacetic acid (diluted in Hanks Balanced Salt Solution (HBSS)) for 3 minutes in a cell culture incubator (37°C, 5% CO₂). After trypsinization, 1000 µL of RPMI complete media were added to each falcon. Islets were centrifuged at 50 x g for 2 minutes and placed in a Round-bottom polystyrene tube.

Islets were infected with 20 Plaque Forming Units per cell (PFU/cell) in free serum RPMI, assuming that a single islet has 1000 cells. Finally, to achieve the optimal lentivirus transduction, islets were incubated at 37°C overnight. The following day, media were changed (Complete RPMI media) and islets were incubated overnight until the experiment.

Flow Cytometry

The efficiency of the transduction was evaluated following the protocol previously described (Jimenez-Moreno et al., 2015) with a Flow Cytometry Analysis. Around 20 islets per condition (Lentivirus Control, Lentivirus CBS, and Lentivirus CTH) were picked and placed in a 5mL Round-bottom polystyrene tube in a final volume of 500 µL of Complete Islets Media. Then, islets were disaggregated using Trypsin- EDTA 1X for 5 minutes at 37°C and centrifuged at 200 x g for 5 minutes. After trypsinization, the endocrine cells were resuspended in PBS and comparing with a non-infected cells the GFP positive cells were estimated using FAC-SCalibur, BD Biosciences, Spain.

Statistical Analysis

Data were analysed by one-way or two-way ANOVA depending on the experiment. All results are reported as mean ± SEM and in all cases, P-values ≤ 0.05 were considered significant. Analyses were performed using GraphPad Prism 7.04.

IV. Results and Discussion

Compound α treatment

The H₂S donor compound α increases metabolic activity and oxygen consumption in pancreatic islets.

Primary islets treated with 5 μ M and 10 μ M of compound α have shown increased MTT activity when compared with the untreated control (Figure 4). MTT test measure indirectly the cellular metabolic activity (viability) by the reduction of the tetrazolium compound (yellow) to water insoluble formazan precipitates (blue-magenta) using NADH/NADPH⁴¹. Formazan crystals can be dissolved using an organic solvent and analyzed colorimetrically⁴².

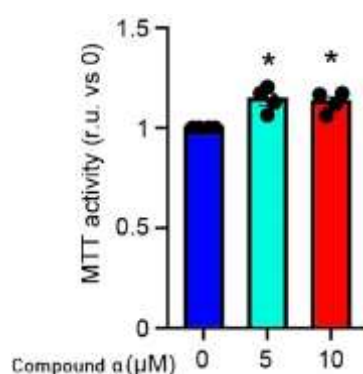


Figure 4. Determination of cell viability in pancreatic islets treated with compound α .

Increased in MTT activity in pancreatic islets treated with 5 and 10 μ M of compound α . n=4. Data shown as mean \pm SEM. * $p \leq 0.05$ vs. Control (one way ANOVA test).

The increase in cell metabolic activity by compound α might be an effect of its activity at the mitochondria. Mitochondria are considered one of the main targets of H₂S effects, having a directly impact on the respiratory chain^{22,43}. Therefore, we measured parameters of mitochondrial function.

We examined mitochondrial performance using Seahorse XF technology in pancreatic islets in response to compound α (Figure 5). We found that *oxygen consumption rate* (OCR) was increased in islets exposed to high concentrations of glucose (22 mM) when treated with compound α at 10 μ M. This technology is based on the inhibition or activation of the different complexes of the respiratory chain, which makes possible the evaluation of parameters such as maximum cellular respiration, basal respiration, or ATP-linked OCR.

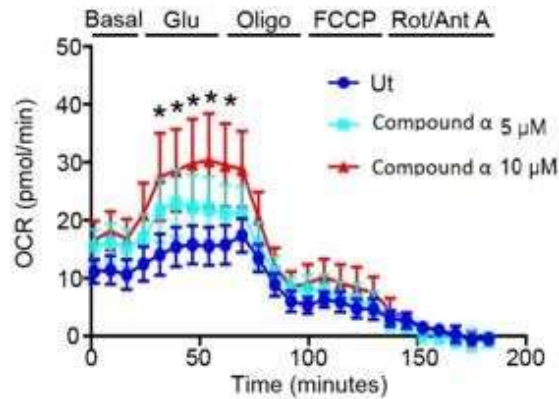


Figure 5. Determination of cellular oxygen consumption.

Oxygen consumption of pancreatic islets treated with 5 and 10 μM of compound α in basal conditions, exposed to high concentrations of glucose (22 mM), and to modulators of respiration (Oligomycin, Carbonyl cyanide-4 (trifluoromethoxy) phenylhydrazone (FCCP), Rotenone, and Antimycin). $n=7$ (Untreated), 6 (Compound α 5 μM), 7 (Compound α 10 μM). Data shown as mean \pm SEM. * $p \leq 0.05$ vs. control (two-way ANOVA test).

As previously mentioned, mitochondria are essential for the production of ATP in the cells⁴⁴. M3dis et al., 2016⁴⁵ showed the existence of a persulfidation mechanism at the level of the respiratory chain, specifically in Complex V (ATP synthase). In this report the authors determined that high levels of H_2S produced an increase in the persulfidation of 2 cysteine residues of ATP5A1. As a consequence, persulfidated ATP5A1 exhibited increased ATP synthase activity when compared with ATP synthase variants lacking persulfidated cysteines (mutations in the target cysteines of persulfidation). The effects of the H_2S donor compound α could be mediated through this mechanism, leading to a marked increase in mitochondrial energy production and cellular respiration on conditions of high glucose concentration in the cell culture media²².

In addition, other mechanisms by which the H_2S donor compound α may be driving an increase in oxygen consumption, is via increased electron flow in the ETC resulting from the oxidation of H_2S by SQOR. These electrons are captured by ubiquinone and transferred to Complex III (Cytochrome C reductase) of the respiratory chain²². This process could also contribute to increase the oxygen consumption and, consequently, ATP production.

The Seahorse XF technology also measures the *extracellular acidification rate* (ECAR). The increase of this biochemical process is indicative of an acidification of the medium produced by the increase of lactic acid and protons resulting from glycolysis. Pancreatic islets showed no

effects in pH on exposure of 10 μM compound α , while there was a significant increase in islets exposed to high concentration of glucose when treated with compound α at 5 μM (Figure 6).

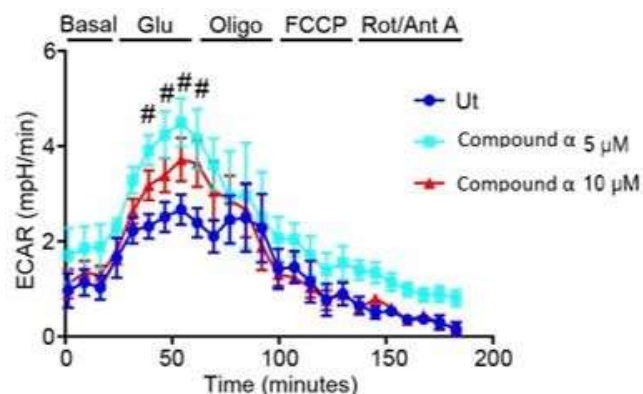


Figure 6. Extracellular acidification of the medium.

Extracellular acidification of the medium of pancreatic islets treated with 5 and 10 μM compound α in basal conditions and when they are exposed to high concentrations of glucose (22 mM) and modulators of respiration (Oligomycin, Carbonyl cyanide-4 (trifluoromethoxy) phenylhydrazone (FCCP), Rotenone, and Antimycin). n=7 (Untreated), 6 (Compound α 5 μM), 7 (Compound α 10 μM). Data shown as mean \pm SEM. * $p \leq 0.05$ vs. control (two-way ANOVA test).

The H₂S donor compound α increases Insulin-secretion in pancreatic islets.

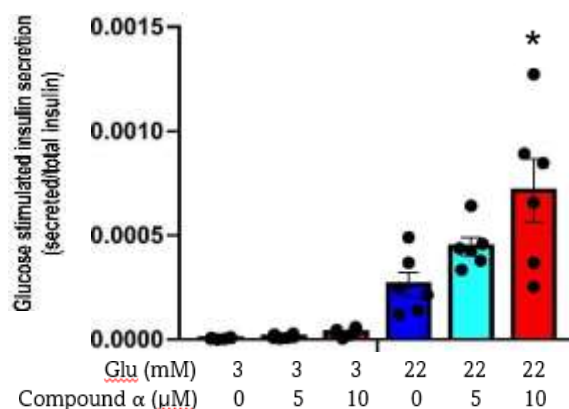


Figure 7. Glucose-promoted insulin secretion.

Increased Insulin secretion of pancreatic islets treated with 10 μM compound α when they are exposed to high glucose (22 mmol/l). n=7. Data shown as mean \pm SEM. * $p \leq 0.05$ vs. control (two-way ANOVA test).

Insulin-secretion tests have determined that under high glucose (22 mM), compound α (10 μM) increased insulin secretion in pancreatic islets (Figure 7). Therefore, the functionality of the pancreatic islets is altered by compound α .

Relative gene expression in pancreatic islets treated with 5 and 10 μ M compound α .

Using the RT-PCR SYBR Green Kit we examined the relative gene expression of the two main enzymes that synthesize H_2S (CBS and CTH), as well as elements of glucose metabolism such as the transmembrane protein transporter that enables the passive movement of glucose across cell membranes (GLUT2), Insulin 1 (INS1), Insulin 2 (INS2) and the phosphorylating enzyme that controls the entry of glucose into the glycolytic pathway (GCK) (Figure 8).

These results are preliminary data because there are not enough replicates available to apply statistics. Additional RT-PCR is required to obtain a larger number of replicates, but preliminarily, it seems that pancreatic islets treated with 5 and 10 μ M compound α increase the relative expression of CTH, INS1 and INS2. The increased relative expression of INS1 and INS2 genes may be to the increased insulin secretion of pancreatic islets.

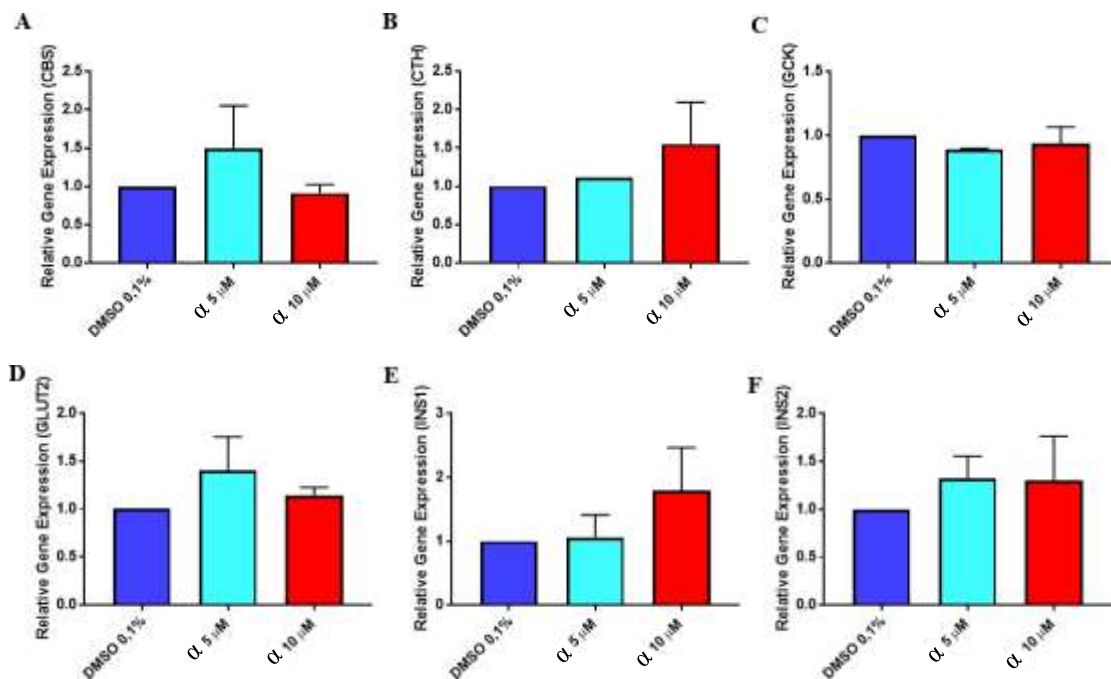


Figure 8. Relative Gene Expression by RT-PCR.

Relative gene expression in pancreatic islets treated with 5 and 10 μ M compound α with repeat-positive reverse transcription polymerase chain reaction (RT-PCR). Expression levels of the housekeeping RSP29 gene were used for normalization. (A) Cystathionine beta synthase expression (CBS); (B) Cystathionine γ -lyase expression (CTH); (C) Glucokinase expression (GCK); (D) Glycotransporter 2 expression (GLUT 2); (E) Insulin 1 expression (INS1); (F) Insulin 2 expression (INS2). Data shown as mean \pm SEM. No statistical analysis for having a small number of replicates to have statistical power.

Lentivirus infection

The production of lentiviruses was performed using the following plasmids:

- Interest plasmid: CBS, CTH or CONTROL (Figure 9).
- Envelope plasmid: pMD2.G (Figure 10).
- Capsid plasmid: psPAX2 (Figure 11).

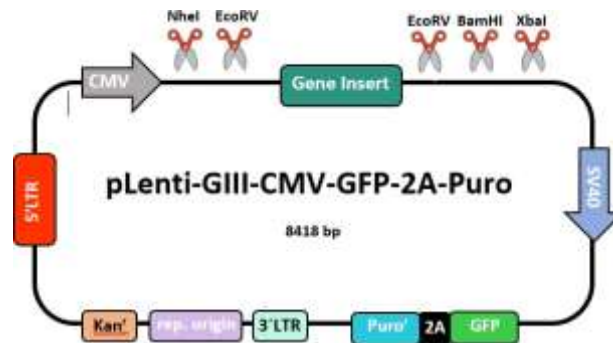


Figure 9. CBS and CTH Lenviral Vector Human (pLenti-GIII-CMV-GFP-2A-Puro).

The CBS, CTH and CONTROL (gene insert) expression is driven by a CMV promoter, with a GFP reporter. The gene inserts are flanked by and can be excised using NheI and BamHI as long as inserts do not contain any internal NheI or BamHI sites.

On the other hand, the envelope plasmid (Figure 10) is a plasmid expressing the VSV-G envelope, whose cloning method is the restriction enzyme.

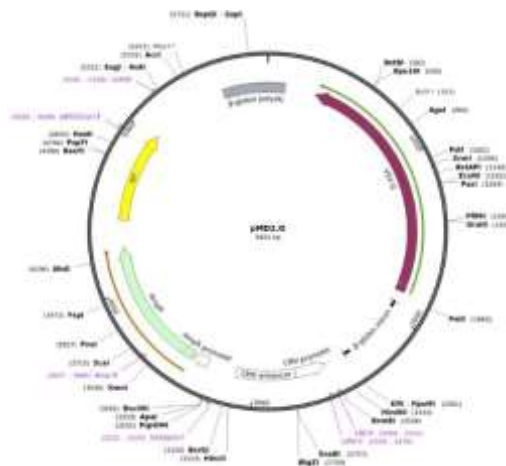


Figure 10. Envelope Plasmid (pMD2.G).

Finally, the plasmid that makes up the viral capsid (Figure 11) is a second-generation lentiviral packaging plasmid, which also features the restriction enzyme as a cloning method.

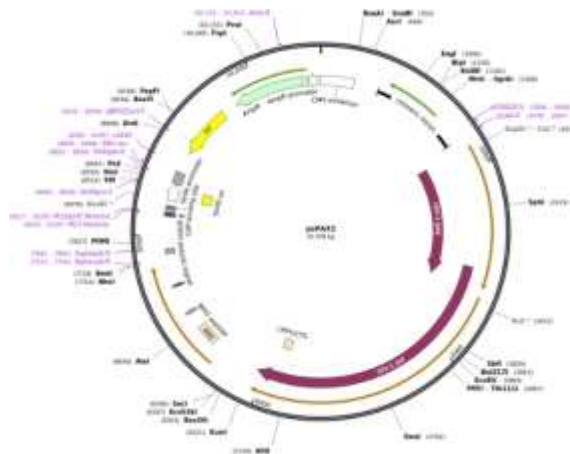
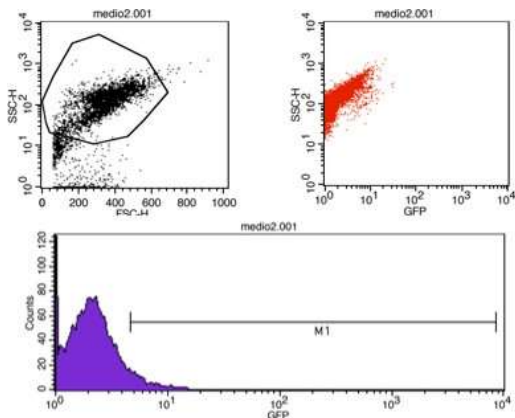


Figure 11. Capsid plasmid (psPAX2).

Viral titer in Hek293T by flow cytometry analysis.

Lentiviral vectors were produced according to the experimental method described in Material and Methods section. The viral titer was validated using Flow Cytometry Analysis in Hek293T cells. Using 10 μ L of each lentivirus condition, **59,35%** of Hek293T were GFP-positive (Figure 12B), **22,45%** for **lentivirus CBS** (Figure 12C) and **35,22%** for **lentivirus CTH** (Figure 12D). These indicated a concentration of viruses of 2,490 x E⁴ Titer Units (TU)/ μ L for lentivirus control, 6,512 x E³ TU/ μ L for lentivirus CBS and 1,008 x E⁴ TU/ μ L for lentivirus CTH.

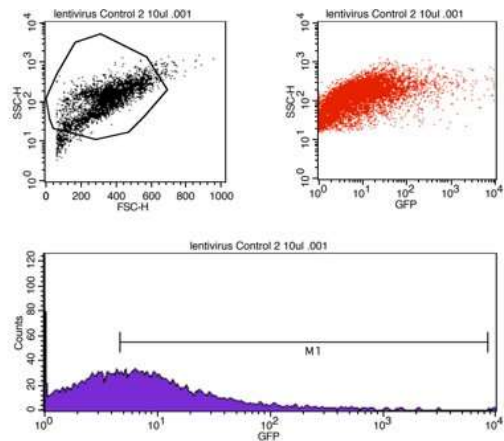
A



File: medio2.001
 Sample ID:
 Gate: G1
 Total Events: 12129
 Log Data Units: Linear Values
 Acquisition Date: 18-Jul-22
 Gated Events: 10000
 X Parameter: GFP (Log)

Marker	Events	% Gated	% Total
All	10000	82.45	82.45
M1	579	5.79	4.77

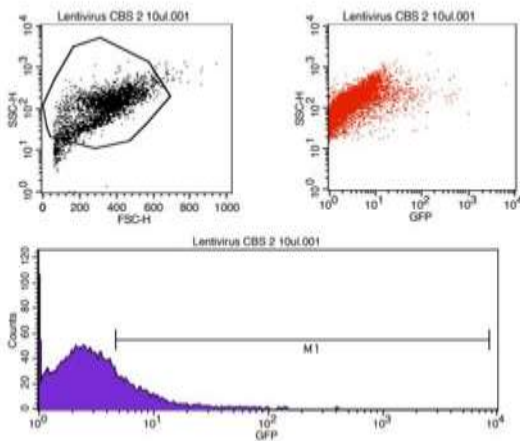
B



File: lentivirus Control 2 10ul .001
 Sample ID:
 Gate: G1
 Total Events: 10813
 Log Data Units: Linear Values
 Acquisition Date: 18-Jul-25
 Gated Events: 10000
 X Parameter: GFP (Log)

Marker	Events	% Gated	% Total
All	10000	92.48	92.48
M1	5935	59.35	54.89

C

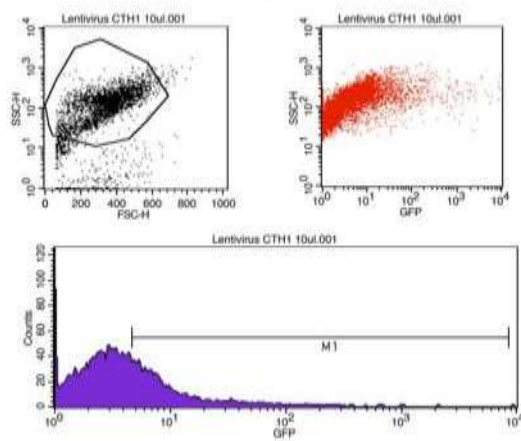


File: Lentivirus CBS 2 10ul.001
 Sample ID:
 Gate: G1
 Total Events: 10691

Log Data Units: Linear Value
 Acquisition Date: 18-Jul-22
 Gated Events: 10000
 X Parameter: GFP (Log)

Marker	Events	% Gated	% Total
All	10000	93.53	91.82
M1	2245	22.45	20.81

D



File: Lentivirus CTH1 10ul.001
 Sample ID:
 Gate: G1
 Total Events: 11370

Log Data Units: Linear Values
 Acquisition Date: 18-Jul-22
 Gated Events: 10000
 X Parameter: GFP (Log)

Marker	Events	% Gated	% Total
All	10000	100.00	87.95
M1	3522	35.22	30.98

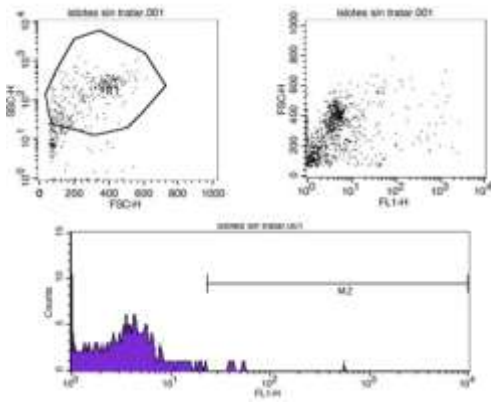
Figure 12. Viral Titer in Flow Cytometry Analysis.

The red circle (% gated) shows the percentage of HEK293T cells that were GFP-positive. Each image was obtained with Flow Cytometry Analysis (FAC-SCalibur, BD Biosciences, Spain) by simply adding 10 μ L of each lentivirus. (A) Media; (B) Lentivirus CONTROL; (C) lentivirus CBS; (D) lentivirus CTH.

Evaluation of the efficiency of infection in pancreatic islets by flow cytometry analysis.

Pancreatic islets were infected using the method described in Materials and Method section using a final concentration of 20 PFU/cell. The efficiency of the transduction in pancreatic islets was evaluated using Flow Cytometry Analysis. **68,92%** of islets were GFP-positive when compared with non-infected cells for **lentivirus control** (Figure 13-B), **42,06%** for **lentivirus CBS** (Figure 13-C) and **47,80%** for **lentivirus CTH** (Figure 13-D). Taken together, these data indicate that the infection protocol was highly efficient.

A

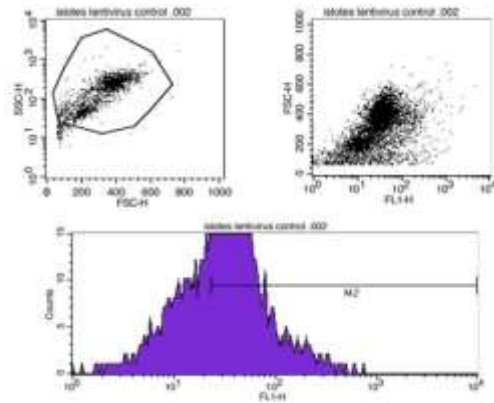


File: isletes sin trator.001
 Sample ID: c-m
 Tube: Untitled
 Acquisition Date: 22-Jul-22
 Gated Events: 823
 X Parameter: FL1-H (Log)

Log Data Units: Linear Values
 Patient ID:
 Panel: Untitled Acquisition Tube List
 Gate: G1
 Total Events: 1336

Marker	Left, Right	Events	% Gated	% Total	Mean	Geo Mean
All	1, 9910	923	7.37	69.14	28.12	4.31
M2	23, 9910	68	5.09	326.59	126.21	

B

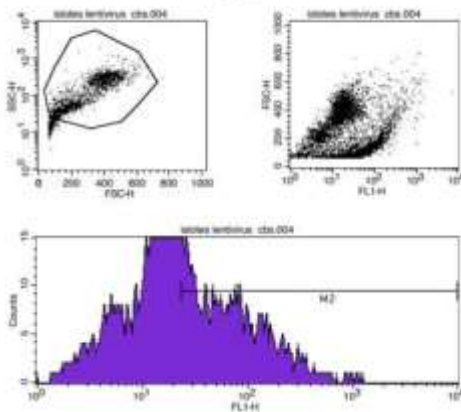


File: isletes lentivirus control.002
 Sample ID: c-m
 Tube: Untitled
 Acquisition Date: 22-Jul-22
 Gated Events: 5000
 X Parameter: FL1-H (Log)

Log Data Units: Linear Values
 Patient ID:
 Panel: Untitled Acquisition Tube List
 Gate: G1
 Total Events: 5248

Marker	Left, Right	Events	% Gated	% Total	Mean	Geo Mean
All	1, 9910	5000	68.92	95.27	52.02	30.84
M2	23, 9910	3446	68.92	65.66	69.75	49.11

C

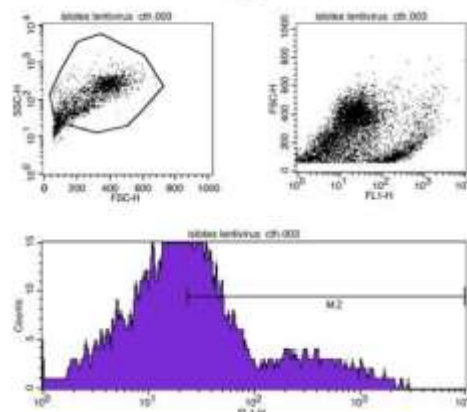


File: isletes lentivirus cbs.004
 Sample ID: c-m
 Tube: Untitled
 Acquisition Date: 22-Jul-22
 Gated Events: 5000
 X Parameter: FL1-H (Log)

Log Data Units: Linear Values
 Patient ID:
 Panel: Untitled Acquisition Tube List
 Gate: G1
 Total Events: 5853

Marker	Left, Right	Events	% Gated	% Total	Mean	Geo Mean
All	1, 9910	5000	42.06	85.43	56.62	23.84
M2	23, 9910	2103	42.06	35.93	117.31	72.28

D



File: isletes lentivirus cth.003
 Sample ID: c-m
 Tube: Untitled
 Acquisition Date: 22-Jul-22
 Gated Events: 5000
 X Parameter: FL1-H (Log)

Log Data Units: Linear Values
 Patient ID:
 Panel: Untitled Acquisition Tube List
 Gate: G1
 Total Events: 5483

Marker	Left, Right	Events	% Gated	% Total	Mean	Geo Mean
All	1, 9910	5000	47.80	91.02	107.39	26.88
M2	23, 9910	2390	47.80	43.51	212.24	86.04

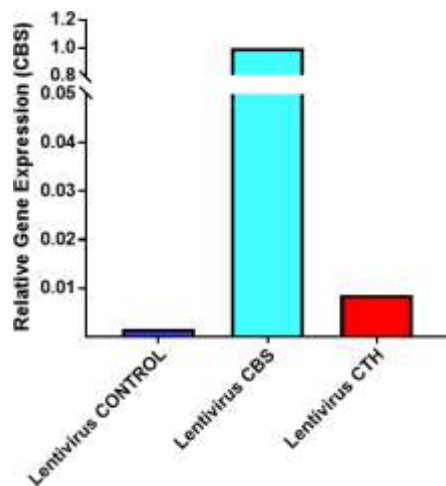
Figure 13. Efficiency of the transduction by Flow Cytometry Analysis.

The red circle (% gated) shows the percentage of pancreatic islets that were GFP-positive. Each image was obtained from Flow Cytometry Analysis (FAC-SCalibur, BD Biosciences, Spain) by adding RPMI Media (A), lentivirus CONTROL (B), lentivirus CBS (C) or lentivirus CTH (D). FL1-H is the digital representation of the fluorescence intensity detected.

Evaluation of the efficiency of infection in pancreatic islets by RT-PCR.

48 hours after the infection, the efficiency of transduction in pancreatic islets was evaluated by RT-PCR using the RT-PCR SYBR Green Kit. Figure 14 shows the level of expression of the CBS (Figure 14-A) and CTH (Figure 14-B) enzyme (target of the lentivirus). Specifically, the CBS lentivirus in pancreatic islets achieves an expression of approximately 600-fold, while the CTH lentivirus achieves an expression of approximately 1000-fold. These expression levels were achieved because the lentiviruses express the CBS and CTH human enzymes. Therefore, expression levels of these enzymes in control islets are unexpected.

A



B

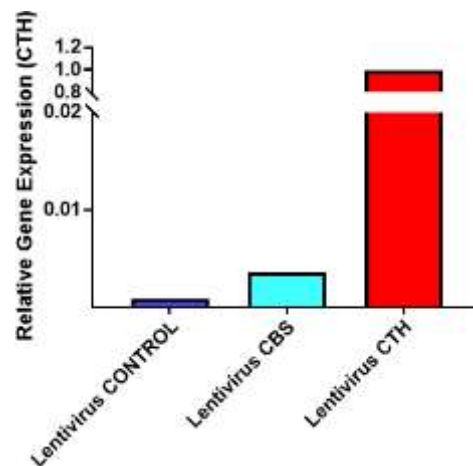


Figure 14. Relative Gene Expression by RT-PCR.

Relative CBS and CTH gene expression in pancreatic islets with an overexpression of CBS and CTH using lentivirus infection with repeat-positive reverse transcription polymerase chain reaction (RT-PCR). (A) Cystathionine beta synthase expression (CBS); (B) Cystathionine γ -lyase expression (CTH). $n=2$. Data shown as mean \pm SEM.

Preliminary data of CBS or CTH overexpression indicates increases in metabolic activity.

Primary islets infected with lentivirus to achieve an overexpression of CBS and CTH showed increased in MTT activity when compared with the lentivirus control (Figure 15). These results are preliminary data because there are not enough replicates available to apply statistics. Additional MTT test is required to obtain a larger number of replicates, but preliminarily, it seems that the overexpression of CBS and CTH, the two main enzymes that synthesized H_2S , increase the production of H_2S in pancreatic islets and this leads to an increase in metabolic activity by its action at the mitochondrial level, specifically in the respiratory chain. For this

reason, in a near future, we are going to study mitochondrial performance using Seahorse XF technology in pancreatic islets overexpressing CTH or CBS.

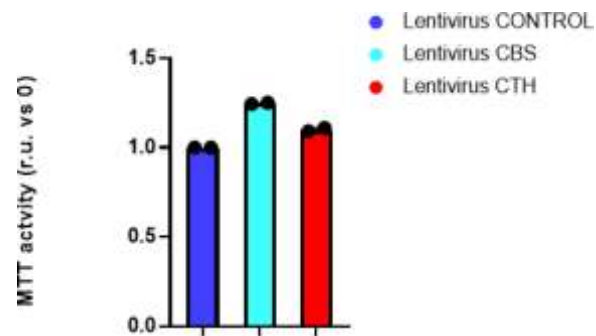


Figure 15. MTT Activity in pancreatic islets infected with lentivirus for 48 hours.

Increased in MTT activity in pancreatic islets infected with lentivirus CBS and CTH in comparison with the control (lentivirus control). n=2. Data shown as mean \pm SEM. No statistical analysis for having a small number of replicates to have statistical power.

V. Conclusions

DM is a major cause of morbidity and mortality and current therapies have not demonstrated to be fully effective. For this reason, we bet on H₂S, a novel gasotransmitter that could play an important role in pancreatic islets.

To modulate the intracellular production of H₂S in these cells, we treated pancreatic islets with a dose of 5 and 10 μM of compound α, a H₂S donor. The pancreatic islets showed increased metabolic activity due to the effect of H₂S at the mitochondria, which was demonstrated by using the technology Seahorse XF. In response to compound α, we found that OCR was increased in islets exposed to high concentrations of glucose. This effect may be the result of a persulfidation of H₂S at the respiratory chain, but further research is required to increase knowledge on the alterations that occur in mitochondria. In addition, pancreatic islets treated with compound α showed increased insulin secretion, suggesting that mitochondrial function and the insulin secretion machinery are coupled.

Furthermore, we also modulate the intracellular production of H₂S overexpressing CBS and CTH in pancreatic islets using a high efficiency protocol of lentivirus infection. These cells also showed increased metabolic activity but, further studies are needed to determine if it is an effect at the mitochondrial level and whether increased insulin secretion also occurs upon CBS or CTH overexpression.

Future studies will focus on insulin secretion and mitochondrial activity of pancreatic islets with CBS and CTH overexpression and using small interfering RNA (siRNA) to achieve opposite effects.

VI. Bibliography

1. Ahlqvist E, Prasad RB, Groop L. Towards improved precision and a new classification of diabetes mellitus. *J. Endocrinol.* 2021; 252(3):R59-R70.
2. Ramírez-Domínguez, M. Pancreatic Islet Isolation. *Adv Exp Med Biol.* 2016; 938:25-34.
3. Xia Z, et al. Long-term effectiveness of group-based diabetes self-management on glycosylated haemoglobin for people with type 2 diabetes in community: a protocol of systematic review and meta-analysis. *BMJ Open.* 2021;11(6):e046692.
4. Jiménez-Moreno CM, et al. A Simple High Efficiency Intra-Islet Transduction Protocol Using Lentiviral Vectors. *Curr Gene Ther.* 2015;15(4):436-46.
5. Siehler J, Blöchinger AK, Meier M, Lickert H. Engineering islets from stem cells for advanced therapies of diabetes. *Nat Rev Drug Discov.* 2021; 20(12):920-940.
6. Wu Y, Ding Y, Tanaka Y, Zhang W. Risk Factors Contributing to Type 2 Diabetes and Recent Advances in the Treatment and Prevention. *Int J Med Sci.* 2014;11(11):1185-200.
7. Mahler RJ, Adler ML. Type 2 Diabetes Mellitus: Update on Diagnosis, Pathophysiology, and Treatment. *J Clin Endocrinol Metab.* 1999; 84(4):1165-71.
8. Kowalska M, Rupik W. Architecture of the Pancreatic Islets and Endocrine Cell Arrangement in the Embryonic Pancreas of the Grass Snake (*Natrix natrix* L.). Immunocytochemical Studies and 3D. *Int J Mol Sci.* 2021; 22(14):7601.
9. Gittes GK. Developmental biology of the pancreas: A comprehensive review. *Devl Biol.* 2009; 326(1):4-35.
10. Muratore M, Santos C, Rorsman P. The vascular architecture of the pancreatic islets: A homage to August Krogh. *Comp Biochem Physiol A Mol Integr Physiol.* 2021; 252:110846.
11. Fuente-Martín E, et al. Dissecting the Brain/Islet Axis in Metabesity. *Genes (Basel).* 2019; 10(5):350.
12. Sheehy DF, Quinnell S, Vegas AJ. Targeting Type 1 Diabetes: Selective Approaches for New *Biochemistry.* 2019; 58(4):214–233.

13. Ahlqvist E, Prasad RB, Groop L. 100 YEARS OF INSULIN: Towards improved precision and a new classification of diabetes mellitus. *J Endocrinol.* 2021; 252(3):R59–R70.
14. Ojo O. Recent Advances in Nutrition and Diabetes. *Nutrients.* 2021; 13(5):1573.
15. Abdulreda MH, et al. The Different Faces of the Pancreatic Islet. *Adv Exp Med Biol.* 2016; 938:11-24.
16. Piragine E, Calderone V. Pharmacological modulation of the hydrogen sulfide (H₂S) system by dietary H₂S-donors: A novel promising strategy in the prevention and treatment of type 2 diabetes mellitus. *Phytother Res.* 2021; 35(4):1817–1846.
17. Gheibi S, Samsonov AP, Gheibi S, Vazquez AB, Kashfi K. Regulation of carbohydrate metabolism by nitric oxide and hydrogen sulfide: Implications in diabetes. *Biochem Pharmacol.* 2020; 176:113819.
18. Zhang H, et al. Hydrogen sulfide regulates insulin secretion and insulin resistance in diabetes mellitus, a new promising target for diabetes mellitus treatment? A review. *J Adv Res.* 2020; 27:19-30.
19. Chen HJ, et al. Role of Hydrogen Sulfide in the Endocrine System. *Front Endocrinol (Lausanne).* 2021; 12:704620.
20. Zhu L, Yang B, Ma D, Wang L, Duan W. Hydrogen Sulfide, Adipose Tissue and Diabetes Mellitus. *Diabetes Metab Syndr Obes.* 2020; 13:1873-1886.
21. Cheng Z, Kishore R. Potential role of hydrogen sulfide in diabetes-impaired angiogenesis and ischemic tissue repair. *Redox Biol.* 2020; 37:101704.
22. Murphy B, Bhattacharya R, Mukherjee P. Hydrogen sulfide signaling in mitochondria and disease. *FASEB J.* 2019; 33(12):13098.
23. Kolluru GK, Shen X, Bir SC, Kevil CG. Hydrogen sulfide chemical biology: Pathophysiological roles and detection. *Nitric Oxide.* 2013; 35:5–20.
24. Rodrigues C, Percival SS. Immunomodulatory Effects of Glutathione, Garlic Derivatives, and Hydrogen Sulfide. *Nutrients.* 2019; 11(2):295.
25. Abe K, Kimura H. The Possible Role of Hydrogen Sulfide as an Endogenous Neuromodulator. *J Neurosci.* 1996; 16(3):1066-71.

26. Wang R. Physiological implications of hydrogen sulfide: A whiff exploration that blossomed. *Physiol Rev.* 2012; 92(2):791–896.
27. Zaorska E, Tomasova L, Koszelewski D, Ostaszewski R, Ufnal M. Hydrogen Sulfide in Pharmacotherapy, Beyond the Hydrogen Sulfide-Donors. *Biomolecules.* 2020; 10(2):323.
28. Gheibi S, et al. Regulation of carbohydrate metabolism by nitric oxide and hydrogen sulfide: Implications in diabetes. *Biochem Pharmacol.* 2020; 176:113819.
29. Landry AP, Ballou DP, Banerjee R. Hydrogen Sulfide Oxidation by Sulfide Quinone Oxidoreductase. *Chembiochem.* 2021; 22(6):949.
30. Landry AP, Ballou DP, Banerjee R. H₂S oxidation by nanodisc-embedded human sulfide quinone oxidoreductase. *J Biol Chem.* 2017; 292(28):11641–11649.
31. Gubern M, Andriamihaja M, Nübel T, Blachier F, Bouillaud F. Sulfide, the first inorganic substrate for human cells. *FASEB J.* 2007; 21(8):1699–1706.
32. Jain S K, et al. Low Levels of Hydrogen Sulfide in the Blood of Diabetes Patients and Streptozotocin-Treated Rats Causes Vascular Inflammation? *Antioxid Redox Signal.* 2010; 12(11):1333-7.
33. Suzuki K, Sagara M, Aoki C, Tanaka S, Aso Y. Clinical Implication of Plasma Hydrogen Sulfide Levels in Japanese Patients with Type 2 Diabetes. *Intern Med.* 2017; 56(1):17–21.
34. Whiteman M, et al. Adiposity is a major determinant of plasma levels of the novel vasodilator hydrogen sulphide. *Diabetologia.* 2010; 53(8):1722-6.
35. Koster JC, Permutt MA, Nichols CG. Diabetes and Insulin Secretion: The ATP-Sensitive K⁺ Channel (KATP) Connection. *Diabetes.* 2005; 54(11):3065–3072.
36. Szeto V, Chen NH, Feng ZP, Sun HS. The role of K ATP channels in cerebral ischemic stroke and diabetes. *Acta Pharmacol Sin.* 2018; 39(5):683–694.
37. Lu A, Chu C, Mulvihill E, Wang R, Liang W. ATP-sensitive K⁺ channels and mitochondrial permeability transition pore mediate effects of hydrogen sulfide on cytosolic Ca²⁺ homeostasis and insulin secretion in β -cells. *Pflugers Arch.* 2019; 471(11-12):1551-1564.

38. Ali MY, Whiteman M, Low CM, Moore PK. Hydrogen sulphide reduces insulin secretion from HIT-T15 cells by a K ATP channel-dependent pathway. *J Endocrinol.* 2007; 195(1):105–112.
39. Yang W, Yang G, Jia X, Wu L, Wang R. Activation of KATP channels by H₂S in rat insulin-secreting cells and the underlying mechanisms. *J Physiol.* 2005; 569:519–31.
40. Brun T, et al. The diabetes-linked transcription factor PAX4 promotes β -cell proliferation and survival in rat and human islets. *J Cell Biol.* 2004; 167(6):1123-35.
41. van Tonder A, Joubert AM, Cromarty AD. Limitations of the 3-(4,5-dimethylthiazol-2-yl)-2,5-diphenyl-2H-tetrazolium bromide (MTT) assay when compared to three commonly used cell enumeration assays. *BMC Res Notes.* 2015; 8:47.
42. Stepanenko AA, Dmitrenko VV. Pitfalls of the MTT assay: Direct and off-target effects of inhibitors can result in over/underestimation of cell viability. *Gene.* 2015; 574(2):193–203.
43. Nicholls P, Marshall DC, Cooper CE, Wilson MT. Sulfide inhibition of and metabolism by cytochrome c oxidase. *Biochem Soc Trans.* 2013; 41(5):1312–6.
44. Plitzko B, Loesgen S. Measurement of Oxygen Consumption Rate (OCR) and Extracellular Acidification Rate (ECAR) in Culture Cells for Assessment of the Energy Metabolism. *Bio Protoc.* 2018; 8(10):e2850.
45. Módis K, et al. S-sulfhydration of ATP synthase by hydrogen sulfide stimulates mitochondrial bioenergetics. *Pharmacol Res.* 2016; 113:116-124.



UNIVERSITY OF SEVILLE

Master Thesis

***Evaluating the modulation of the intracellular
production of H₂S in the functionality and metabolic activity of primary
cultures of pancreatic islets***

Master in Biomedical Research

Andalusian Center of Molecular Biology and Regenerative Medicine



21 February 2022 – 5 September 2022

Inmaculada Pino Pérez

In Seville, 5 of September of 2022

Tutor: Alejandro Martín-Montalvo Sánchez

Co-tutor: Iván Valle Rosado

Date of the defense: 22 of September of 2022